Paramyotonia Congenita Mutations Reveal Different Roles for Segments S3 and S4 of Domain D4 in hSkM1 Sodium Channel Gating

Sen Ji,* Alfred L. George, Jr.,§ Richard Horn,‡ and Robert L. Barchi*

From the *Departments of Neurology and Neuroscience and the Mahoney Institute of Neurological Sciences, University of Pennsylvania School of Medicine, Philadelphia, Pennsylvania 19104-6074; ‡Department of Physiology, Jefferson Medical College, Philadelphia, Pennsylvania 19107; and §Departments of Medicine and Pharmacology, Vanderbilt University School of Medicine, Nashville, Tennessee 37232

ABSTRACT Mutations in the gene encoding the voltage-gated sodium channel of skeletal muscle (SkM1) have been identified in a group of autosomal dominant diseases, characterized by abnormalities of the sarcolemmal excitability, that include paramyotonia congenita (PC) and hyperkalemic periodic paralysis (HYPP). We previously reported that PC mutations cause in common a slowing of inactivation in the human SkM1 sodium channel. In this investigation, we examined the molecular mechanisms responsible for the effects of L1433R, located in D4/S3, on channel gating by creating a series of additional mutations at the 1433 site. Unlike the R1448C mutation, found in D4/S4, which produces its effects largely due to the loss of the positive charge, change of the hydropathy of the side chain rather than charge is the primary factor mediating the effects of L1433R. These two mutations also differ in their effects on recovery from inactivation, conditioned inactivation, and steady state inactivation of the hSkM1 channels. We constructed a double mutation containing both L1433R and R1448C. The double mutation closely resembled R1448C with respect to alterations in the kinetics of inactivation during depolarization and voltage dependence, but was indistinguishable from L1433R in the kinetics of recovery from inactivation and steady state inactivation. No additive effects were seen, suggesting that these two segments interact during gating. In addition, we found that these mutations have different effects on the delay of recovery from inactivation and the kinetics of the tail currents, raising a question whether this delay is a reflection of the deactivation process. These results suggest that the S3 and S4 segments play distinct roles in different processes of hSkM1 channel gating: D4/S4 is critical for the deactivation and inactivation of the open channel while D4/S3 has a dominant role in the recovery of inactivated channels. However, these two segments interact during the entry to, and exit from, inactivation states.

INTRODUCTION

Abnormalities in the skeletal muscle voltage-gated sodium channel (SkM1), a protein essential for generation of the action potential in sarcolemma, can have important consequences for muscle contraction (Barchi, 1995). Such consequences are exemplified by a group of autosomal dominant hereditary muscle diseases, including paramyotonia congenita (PC) and hyperkalemic periodic paralysis (HYPP), in which symp-

toms can be attributed to either hyperexcitability or hypoexcitability of the sarcolemma. The relationship of these diseases to the sodium channel in skeletal muscle was first suggested by the identification of a tetrodotoxin (TTX)-sensitive, noninactivating inward current in muscle fibers obtained from patients having PC or HYPP. A causal relationship between defects in sodium channels and these diseases was established when genetic linkage analysis showed both HYPP and PC to be allelic disorders of the human adult skeletal muscle sodium channel α subunit (hSkM1) gene (*SCN4A*). So far 16 point mutations, widely distributed throughout the primary sequence of domains 2 to 4 of the hSkM1 sodium channel, have been reported in PC and HYPP patients (Barchi, 1995; Ji et al., 1995).

Address correspondence to R. L. Barchi, Institute of Neurological Sciences, 218 Stemmler Hall, University of Pennsylvania School of Medicine, Philadelphia, PA 19104-6074.

Previously, we reconstructed five PC mutations (A1156T, T1313M, L1433R, and R1448C/H) in the hSkM1 background and found that these mutations, when expressed in a mammalian cell line (tsA 201), share a common pattern of alterations in channel gating that includes slowing of the rate of inactivation and acceleration in the rate of recovery from inactivation, although they differ in their effects on the voltage dependence of these processes (Yang et al., 1994). The slowing of inactivation that is characteristic of PC mutations is distinguishable from the appearance of an abnormal slow gating mode reported in HYPP mutations. At the single-channel level, R1448C/H mutations inactivate poorly, with a greatly reduced rate constant for inactivation from the open state (Chahine et al., 1994).

All of the mutations reported in HYPP and PC pedigrees are point mutations that introduce single amino acid substitutions (Barchi, 1995). Although these mutations are spread throughout repeat domains D2 to D4, all that have been expressed (Chahine et al., 1994; Cannon and Strittmatter, 1993; Cummins et al., 1993; Yang et al., 1994) have profound effects on sodium channel inactivation, suggesting that multiple regions of the channel structure are involved in normal inactivation. The mechanisms by which each mutation affects inactivation, and the responsible properties of the amino acid side chain, in most cases remain to be determined.

We have previously proposed that the loss of positive charge on R1448 is largely responsible for the effects on inactivation in the R1448C/H mutations. Since L1433R also involves a change of charge, we wondered whether a similar mechanism might be involved in its effects on inactivation. Furthermore, since these two mutations are located in adjacent regions of the secondary structure, examination of interactions between them could shed light on the functional relationships that exist between the segments in which they are found.

In the work reported here, we address these questions by introducing a series of mutations at L1443 and by examining a double mutation containing both L1433R and R1448C (Ptáček et al., 1992, 1993). We find that the addition of a positive charge at 1433 is not an essential factor in slowing inactivation. Instead, a change in the hydropathy of the side chain appears to be more important. Additionally, L1433R and R1448C mutations differ significantly in the effects on different gating processes, suggesting different roles for D4/S3 and D4/S4. More interestingly, L1433R and R1448C interact with each other in a nonadditive pattern. Our data also call into question whether the delay in recovery from inactivation is a reflection of deactivation, since these two processes are affected differently by these mutations.

MATERIALS AND METHODS

Mutagenesis

Site-directed mutagenesis experiments were performed using the pSELECT Mutagenesis System (Promega Corp., Madison, WI) as previously described (Chahine et al., 1994). Antisense mutagenic oligonucleotides were as follows: L1433Q/E/K, 5'-gatcaggtcagatt[g,c,t]ggcaaggcccacaat-3' (square brackets define mixed synthesis sites, mutagenic sequence is underlined); L1433A, 5'-gatcaggtcagaggcggcaaggcccacaat-3'; L1433M, 5'-gatcaggtcagacatggcaaggcccac-3'. The three mutations L1433Q, L1433E, and L1433K were made in a single reaction by using a degenerative mutagenic primer, and later identified by nucleotide sequencing of multiple independent recombinants. All sequence verified mutants were assembled into the mammalian expression construct pRc/CMV-hSkM1. The mutations L1433R and R1448C were made previously (Chahine et al., 1994; Yang et al., 1994).

The double mutant L1433R/R1448C was assembled by ligation of a 1.75-kb XmnI/XbaI fragment from pRc/CMV-R1448C containing the R1448C mutation into the corresponding restriction sites of the pRc/CMV-L1433R construct. The presence of both mutations in the final construct was verified by DNA sequence analysis.

Transfection of cDNAs into tsA Cells

The conventional $CaPO_4$ transfection method was employed in the transfection of tsA 201 cells with recombinant DNAs, as reported previously (Chahine et al., 1994). In brief, tsA 201 cells growing in 100-mm tissue culture dishes at 30–50% confluence were transfected with 15 μg of each plasmid cDNA encoding hSkM1 wild-type (wt) or mutant sodium channels after the formation of precipitates with $CaPO_4$. $CaPO_4$ precipitate was washed out after 12-h incubation at 37°C. About 30–50% of the cells expressed detectable sodium current 18 h after transfection, and the current peaks at 24–72 h. Cells expressing 1–5 nA current at −10 mV depolarization from a holding potential of −90 mV were used for experiments.

Electrophysiological Recordings

The standard whole-cell patch clamp recording configuration (Hamill et al., 1981) was used to record sodium current from the transfected tsA cells. Briefly, an Axopatch-1B patch clamp amplifier (Axon Instruments, Foster City, CA) was interfaced with a PC-type computer through a TL-1 DMA Interface board (Axon Instruments). Data were acquired and analyzed using the pCLAMP software package (Axon Instruments). Recording pipettes were fabricated from Corning 8161 glass (Wilmad Glass Co., Buena, NJ) and had a tip resistance of 0.5–2.0 MΩ when filled with our internal solution. The series resistance was corrected by ~80%. The typical error in the clamp potential caused by this resistance was <3 mV. The liquid junction potentials were not corrected. The recording chamber was bathed with a modified Tyrode's solution containing (in millimolar): 150.0 NaCl, 4.5 KCl, 1.0 $CaCl_2$, 1.0 $MgCl_2$, 10.0 HEPES, and 10.0 glucose, with a pH of 7.4, titrated with NaOH. The patch electrode contained (in mM): 120.0 CsF, 20.0 NaCl, 5.0 EGTA, and 10.0 HEPES. All the recordings were made at a room temperature of 22°C except tail current recordings that were made at 11.9°C. In the latter ex-

periments the temperature was regulated by a TC-10 controller (Dagan Corp., Minneapolis, MN) connected to Peltier units.

Data Analysis

Whole-cell current recordings were analyzed using pCLAMP and SigmaPlot (Jandel Scientific Software, San Rafael, CA) software. All data in both figures and text are expressed as mean ± SEM.

The inactivation time constants (τ_h) were obtained by fitting the inactivating phase of current traces to a single exponential: $I(t) = A \cdot \exp(-t/\tau_h) + A_\infty$. Single exponentials provided good fits for all the mutants. Activation (g/g_{max}) and steady state inactivation (I/I_{max}) curves were obtained by fitting normalized peak currents to Boltzmann relationships:

$$g/g_{max} = 1/\{1 + \exp[ze(V_{1/2} - V)/kT]\},$$

or

$$I/I_{max} = 1/\{1 + \exp[ze(V - V_{1/2})/kT]\},$$

where V is the membrane potential, z is the apparent gating charge, $V_{1/2}$ is the midpoint for current activation or steady state inactivation, and $kT/e = 25$ mV at 22°C. Instantaneous I-V curves were not obtained for these currents. Time constants for recovery (τ_{rcv}) from inactivation were obtained from:

$$I(t) = 1 - \exp(-t/\tau_{rcv}).$$

The time constants (τ_{rcv}) were then fit to:

$$\tau_{rcv}(V) = \tau_{rcv}(0)*\exp(zeV/kT),$$

to obtain the apparent gating charges associated with recovery from inactivation. For conditioned inactivation, normalized peak currents were fit to a single exponential:

$$I/I_{max} = I_\infty - (I_\infty - I_0)*\exp(-t/\tau),$$

to obtain time constants.

RESULTS

Effects of Mutations at 1433 in D4/S3 on hSkM1 Sodium Channel Gating

When expressed in hSkM1, the primary effect of the L1433R mutation is a slowing of sodium channel inactivation (Fig. 1), an effect shared by the other PC mutations that we have studied (Chahine et al., 1994; Yang et al., 1994). Since arginine and leucine differ in charge, hydropathy and size of their side chain, alteration in any of these properties could account for the effects on inactivation. We therefore constructed five additional mutations (L1433A, M, E, K, and Q) to probe the mechanisms underlying the L1433R effects. All of these mutations produce functional sodium channels when transfected in tsA 201 cells in culture. None of the mutations had a significant effect on activation at the whole-cell current level (Figs. 1 A and 3), but varying degrees of slowing in inactivation were observed. This suggests that the alterations of inactivation

kinetics are not secondary to changes in activation kinetics.

Our previous work on R1448C suggested that neutralization of the positive charge is important for the abnormality of inactivation seen with that D4/S4 mutation (Chahine et al., 1994). Since L1433 and R1448 are predicted to reside near the external surface of D4/S3 and D4/S4 respectively, the addition of a positive charge in L1433R could also be crucial for the effect of this mutation. However, we find that charge is not the determining factor here, since the oppositely charged mutations L1433K and L1433E slowed inactivation to a similar degree ($\tau_{h,-10}$: 1.9 and 1.5 ms for L1433K and L1433E vs 0.8 ms for wt) and the neutral polar glutamine (L1433Q) had an even greater effect ($\tau_{h,-10}$: 3.0 ms) (Fig. 1 and Table I). We then probed the effects of a change in hydropathy. The most hydrophilic residue R caused the greatest slowing in channel inactivation,
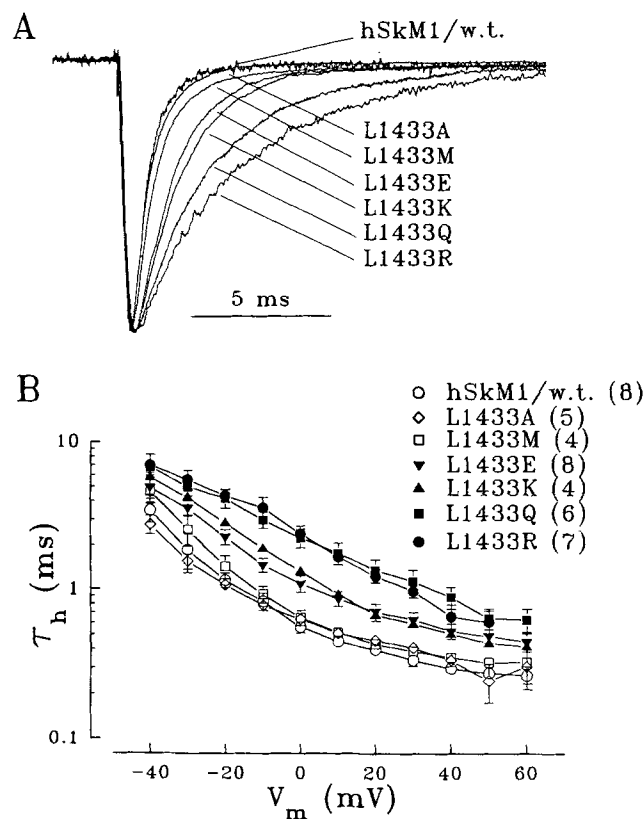

FIGURE 1. Effects of natural and designed mutations at L1433 on hSkM1 sodium channel inactivation. (A) Normalized current traces recorded at −10 mV from a holding potential of −90 mV. Note the differences in the inactivation phase of the current traces among different mutant and wild type hSkM1 channels. (B) Inactivation time constants (τ_h's). Inactivation time constants were obtained by fitting the inactivation phase of current traces recorded from −40 to 60 mV in steps of 10 mV to a single exponential decay. τ_h's at −10 mV depolarization (τ_{h-0}) are summarized in Table I.

TABLE I
Effects of Mutations at 1433 (S3 in D4) and 1448 (S4 in D4) on the Gating of hSkM1 Sodium Channel

	Inactivation (τ_h)		Recovery		Steady state inactivation	
	$\tau_{h,-10}$	z	$\tau_{rcv,-90}$	z	$V_{1/2}$	z
hSkM1/wt (n = 8)	0.82 ± 0.13	1.34 ± 0.16	6.25 ± 0.60	1.74 ± 0.25	−68.28 ± 2.09	4.69 ± 0.22
L1433A (n = 5)	0.77 ± 0.05	0.76 ± 0.11	5.88 ± 0.51	1.39 ± 0.09	−65.04 ± 2.96	4.71 ± 0.18
L1433M (n = 4)	0.91 ± 0.12	1.77 ± 0.12	5.25 ± 0.42	1.44 ± 0.05	−67.05 ± 1.43	5.19 ± 0.23
L1433E (n = 8)	1.45 ± 0.16	1.99 ± 0.13	5.08 ± 0.10	1.15 ± 0.06	−56.65 ± 2.85	4.01 ± 0.19
L1433K (n = 4)	1.89 ± 0.09	0.98 ± 0.10	2.19 ± 0.17	1.19 ± 0.06	−54.79 ± 1.75	3.59 ± 0.10
L1433Q (n = 6)	2.99 ± 0.38	0.68 ± 0.11	2.15 ± 0.22	0.97 ± 0.10	−57.98 ± 2.77	3.41 ± 0.11
L1433R (n = 7)	3.63 ± 0.61	0.71 ± 0.17	2.29 ± 0.67	0.75 ± 0.10	−58.62 ± 4.59	4.10 ± 0.09
R14488C (n = 4)	3.58 ± 0.73	0.12 ± 0.14	2.95 ± 0.30	0.61 ± 0.05	−80.39 ± 0.95	1.87 ± 0.04
L1433R + R1448C (n = 8)	3.75 ± 0.57	0.22 ± 0.23	1.78 ± 0.10	0.74 ± 0.04	−59.70 ± 2.15	2.76 ± 0.17

$\tau_{h,-10}$ (ms): inactivation time constant at a depolarization potential of −10 mV; z (elementary charge, e_0): apparent gating charges; $\tau_{rcv,-90}$ (ms): recovery time constant at −90 mV; $V_{1/2}$ (mV): voltage of 50% inactivation. Each value represents mean ± SEM of four to eight experimental results.

while the hydrophobic alanine and methionine had very little effect. The propensities of alanine and methionine to form α helices are similar to that of leucine (Blaber et al., 1993). Glutamic acid and lysine, which have hydropathy properties intermediate between alanine and arginine (Kyte and Doolittle, 1982), had intermediate effects on inactivation (Fig. 1). However, the degree of the effects did not exactly match the order of relative hydropathy: the polar, noncharged glutamine had a greater effect on τ_h than lysine and glutamic acid. The size of the side chain has less importance in producing an effect on inactivation, although the smallest alanine had the least effect and the largest arginine had the greatest effect (Fig. 1).

In addition to a slowing of inactivation, mutations L1433K/E/Q/R also decreased the voltage dependence of τ_h, with a reduction of apparent gating charge of 0.3 to 0.6 e_0 over a voltage range of −30 to 0 mV (Fig. 1 B and Table I). However, we did not observe a complete loss of the voltage dependence of τ_h in this voltage range, as seen in R1448C/H mutations (see Fig. 4), suggesting that the mutations at L1433 and R1448 interfere with inactivation through different mechanisms.

The recovery from inactivation was faster ($\tau_{rcv} < 5.0$ ms at a potential of −90 mV) in all the mutations at L1433 that slowed inactivation (L1433K/E/Q/R) (Fig. 2 A), as compared with the wild-type channel, ($\tau_{rcv}, _{-90} = 6.3$ ms), suggesting a destabilization of the inactivated state, as we have proposed previously (Chahine et al., 1994), or an acceleration of deactivation and subsequent recovery, or both. Besides acceleration in the recovery from inactivation, L1433 mutations also altered its voltage dependence, with decreases of the apparent gating charges ranging between 0.5 and 1.0 e_0. This de-

crease is most prominent in the natural mutation L1433R, ∼1.0 e_0.

Consistent with the observed changes in development of inactivation (slowed) and recovery from inactivation (accelerated), the steady state inactivation curve (h_∞) was shifted in the depolarized direction for all mutations of L1433 (Fig. 2 B). In other words, the probability that a channel is available to open at a given potential is greater in mutant channels than in wt channels. This is in sharp contrast with the hyperpolarized shift of the h_∞ curve produced by the R1448C/H mutations (Fig. 4 D), suggesting that mutations at these two locations selectively affect different aspects of the inactivation process. Among the amino acids used to replace L1433, the small hydrophobic alanine and methionine mutations had very little effect on steady state inactivation (no significant alteration in either $V_{1/2}$ or the apparent gating charge), while the bulky, charged arginine mutation had the greatest effect ($V_{1/2}$ was shifted by 20 mV) (Table I). In general, changes of the apparent gating charge were not large, except in the L1433Q mutation that showed a reduction of 1.3 e_0.

In spite of the prominent effects on inactivation by several of these mutations (L1433E/K/Q/R), they did not modify activation significantly. This is shown by the superimposition of I-V relation curves of all six mutations with that of the wt channel in Fig. 3 A. Additionally, neither the voltage dependence nor the kinetics of activation was notably altered, as expressed in either the normalized activation curves or the half time for activation curves (Fig. 3, B and C), suggesting that this region in D4/S3 does not play a significant role in activation. Furthermore, the consistency of the reversal potential among different channels (Fig. 3 A) indicates that ionic selectivity is unaltered, suggesting that L1433
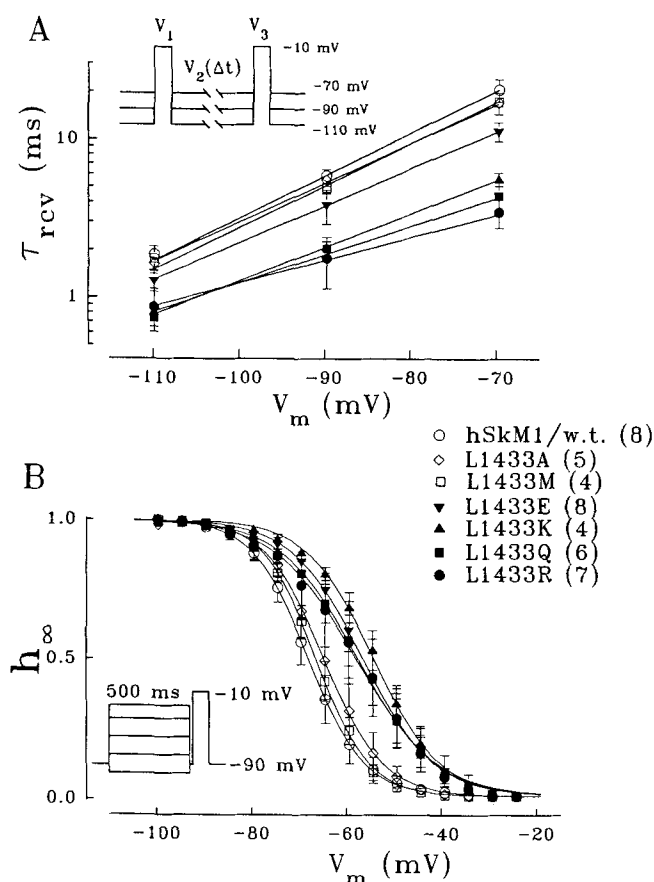
FIGURE 2. Effects of natural and designed mutations at L1433 on hSkM1 recovery from inactivation and steady state inactivation. (A) Time constants of recovery from inactivation at different holding potentials of wt and mutant channels. Recovery from inactivation was measured using a double pulse protocol (inset). Recovery time constants (τ_{rcv}) were obtained by fitting the normalized recovering currents to a single exponential. τ_{rcv}'s at a holding potential of −90 mV and the apparent recovery gating valences are summarized in Table I. (B) Steady state inactivation curves of different natural and designed mutant hSkM1 channels. Steady state inactivation was estimated by measuring currents using a double-pulse protocol (inset). The solid curves are the best fits of the normalized currents to a Boltzmann relationship. $V_{1/2}$'s and the apparent gating valences are summarized in Table I.

is probably not located near the selectivity filter of the pore.

Effects of the Double Mutation (L1433R + R1448C)

Although both L1433R and R1448C mutations slow the rate of inactivation, the two differ in their effects on the voltage-dependence of τ_h, on the rates of the recovery from inactivation, and on steady state inactivation (Fig. 4), suggesting that these mutations generate their effects through different pathways. The putative tertiary structure of the hSkM1 sodium channel (George et al., 1992) suggests that both mutated residues are located

in proximity near the outer ends of S3 and S4 of D4, raising the possibility that mutations at the two sites might be next to, and interact with, each other. To test this idea, we constructed a double mutation containing both L1433R and R1448C and examined the effects of the double mutation on channel gating. As shown in Fig. 4 A (currents recorded at a depolarization of −10 mV), the primary effect of the double mutation is slowing of inactivation. However, the double mutation resembled R1448C more than L1433R in slowing channel inactivation and reducing the voltage dependence of inactivation (Fig. 4 B and Table I). No obvious additive effect was noted, suggesting that the R1448C mutation prevails over L1433R by affecting a rate-limiting step in the inactivation process. Nevertheless, the double mutation surprisingly resembled L1433R rather than R1448C in its effects on the kinetics of recovery from inactivation (Fig. 4 C), suggesting that conformational changes involving S3 may be critical for the recovery process. Since L1433R and R1448C shift the steady state inactivation curve in opposite directions by more than 10 mV, the shift produced by the double mutation (L1433R+R1448C) is particularly interesting. In the L1433R+R1448C channel, the h_∞ curve is shifted in the depolarized direction and superimposes on the curve for L1433R, suggesting a dominating role for S3 in steady state inactivation of hSkM1 channels. $V_{1/2}$ was −60, −59, and −80 mV and the apparent gating charges were 2.8, 4.1, and 1.8 e_0 for the double mutation, L1433R and R1448C, respectively.

The opposite shifts in the steady state inactivation curves produced by L1433R and R1448C mutations could reflect different inactivation rates from the closed states for the two mutations at more negative membrane potentials (e.g., < −50 mV) since sodium channels need not open to inactivate (Horn et al., 1981). In other words, the mutations may affect inactivation from the closed states differently, with L1433R having a stronger effect on this process. The double mutation, R1448C, and L1433R mutations were, therefore, tested for their effects on conditioned inactivation using a double-pulse protocol (inset in Fig. 5). Shown in Fig. 5, A and B are the normalized peak currents from hSkM1/wt and double mutant channels. Normalized peak currents from L1433R and R1448C mutant channels are not shown. Time constants of conditioned inactivation, obtained by fitting the normalized currents to a single exponential relaxation, are shown in Fig. 5 C. All three mutations have much smaller inactivation time constants at membrane potentials more negative than −40 mV, but larger time constants at more positive membrane potentials. At negative voltages, the double mutation does not resemble the L1433R, however. Rather, it has an effect quantitatively greater than the addition of effects of the L1433R and
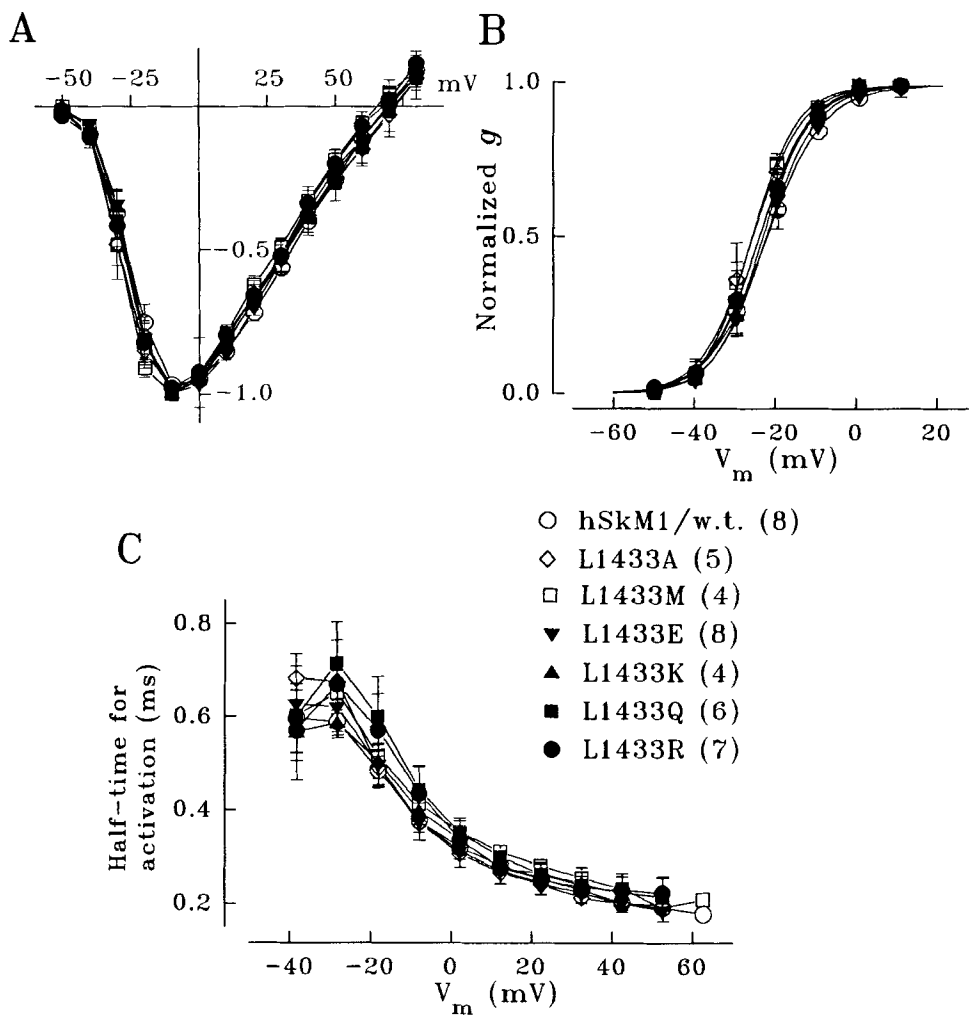
FIGURE 3. L1433 mutations have no significant effects on the voltage dependence and kinetics of sodium current activation. (A) Current-voltage relationship curves of different mutations. Current was recorded from a holding potential of −90 mV by depolarizing the membrane from −50 to 80 mV in steps of 10 mV. Note that the overall shapes of the curves are very similar to each other and that the reversal potentials are about the same, as compared with wt channels. (B) Normalized activation curves. Normalized whole-cell conductances were obtained by dividing the peak currents by the driving force. Solid curves are the best fits to a Boltzmann relationship. $V_{1/2}$'s and the apparent gating valences are summarized in Table I. (C) Half-time for activation curves. Half-time for activation was measured as the time between the onset of the depolarizing pulse and the time when the current reached half of its peak value. Curves are superimposible for different mutations with wt channels.

O hSkM1/w.t. (8)
◇ L1433A (5)
□ L1433M (4)
▼ L1433E (8)
▲ L1433K (4)
■ L1433Q (6)
● L1433R (7)

R1448C, indicating that both mutations have an effect on the entry of the channel into the inactivated states before opening. It is likely, therefore, that both S3 and S4 of D4 participate in closed channel inactivation.

Effects of L1433R, R1448C, and Double Mutation on Deactivation

One mechanism that might contribute to the observation that the double mutation resembles L1433R rather than R1448C in recovery from inactivation and steady state inactivation would be that D4/S3 plays a critical role in the deactivation of the channel and this must precede the recovery process (Patlak, 1991; Kuo and Bean, 1994). If we hypothesize that sodium channels must deactivate before recovery (Kuo and Bean, 1994), mutations in the D4/S3 could influence the rate of recovery by altering the kinetics of deactivation. If this were true, deactivation would be more affected by the L1433R and double mutations than by the R1448C mutation.

To assess this possibility, we measured the delay in

the recovery from inactivation, using a double-pulse protocol (inset of Fig. 6 A), expecting a more pronounced shortening of the delay in the L1433R and double mutant channels than in the R1448C mutation. Our data (Fig. 6) show that the delay in recovery is shorter for mutant channels than for wt channels. For example, there was no significant current recovery between 0.4–0.9 ms (depending on the membrane potential) in the wt channels, whereas recovery was detectable in mutant channels after a delay as short as 0.1–0.3 ms. By the last recovery pulse (1.6 ms of repolarization), only 15% current recovered in wt channels, but over 50% current recovered in mutant channels. Fig. 7, A and B show the normalized recovery curves at a membrane potential of −70 and −100 mV. It is obvious that mutant channels not only have a shorter delay but also recover faster. Shown in Fig. 7 C is the delay plotted against membrane potential. It is apparent that the delays in all three mutant channels are quite similar to each other and have a similar voltage dependence, indicating that the gating process underlying the delay is about equally affected by these mutations. Taken to-
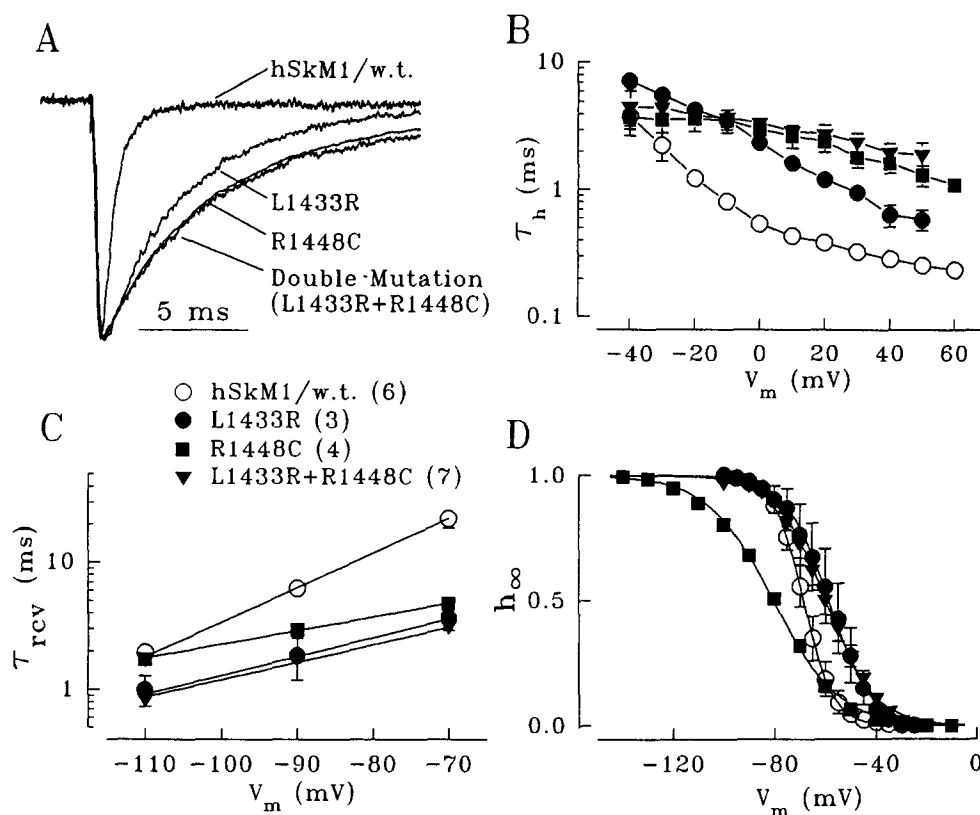
FIGURE 4. Effects of double mutation (L1433R + R1448C) on hSkM1 channel gating. (A) Normalized current traces recorded at -10 mV from a holding potential of -90 mV in wt, double mutation, L1433R, and R1448C channels. (B) Inactivation time constants curve (τ_h's). The double mutation resembles R1448C very closely. (C) Recovery time constants at different holding potentials. The double mutation resembles L1433R mutation very closely. (D) Steady state inactivation curves. The double mutation resembles L1433R.

gether, these data suggest either that both S3 and S4 are involved in deactivation, or that this delay does not reflect the deactivation process.

To further clarify these two possibilities, we examined deactivation kinetics directly by recording tail currents (Fig. 8, A and B). Fig. 8 C shows the time constants of tail currents recorded at repolarization potentials from -130 to -70 mV in 10-mV steps. These experiments were done at 11.9°C to slow the gating kinetics. Surprisingly, the changes in the time constants of tail currents are inconsistent with alterations in the delays of current recovery. Although the mutations decreased both delays in recovery and the time constants of recovery, they increased the deactivation time constants, if they affected deactivation. The double mutant slowed the tail current the most, R1448C mutation less, and L1433R mutation did not show a difference from the wt channel. Therefore, the R1448C mutation in S4 affects the closing of an open channel, but L1433R in S3 does not, again indicating that these two regions play different roles in hSkM1 channel gating. One possibility is that D4/S4 movement is coupled to activation very tightly, but D4/S3 movement is secondary to that of D4/S4. This inconsistency between changes in the tail current kinetics and the delay of recovery raises a question whether these two processes are the same.

DISCUSSION

The α subunit of the human tetrodotoxin-sensitive isoform of sodium channel found in skeletal muscles (hSkM1) is composed of 1836 amino acids and resembles all other known sodium channels in having a putative structure of four domains (D1-D4), each of which contains six hypothesized transmembrane segments (S1-S6) (George et al., 1992). Although structure-function models have been proposed, based largely on the primary sequence of sodium channels (Guy and Seetharamulu, 1986), the functions played by various structural elements remain to be fully defined. The point mutations in the hSkM1 sodium channel identified in PC and HYPP, which alter channel function in vivo, provide us with a unique opportunity to explore the functional role of specific structural regions in channel gating (Chahine et al., 1994; Cannon and Strittmatter, 1994; Ji et al., 1995; Yang et al., 1994). The data presented here suggest that S3 and S4 in D4 play different roles in channel gating, and that mutations L1433R and R1448C in these two segments affect inactivation through different molecular mechanisms. Furthermore, we find that these regions may interact with each other. We further raise questions on the relationship between deactivation and recovery from inactivation.
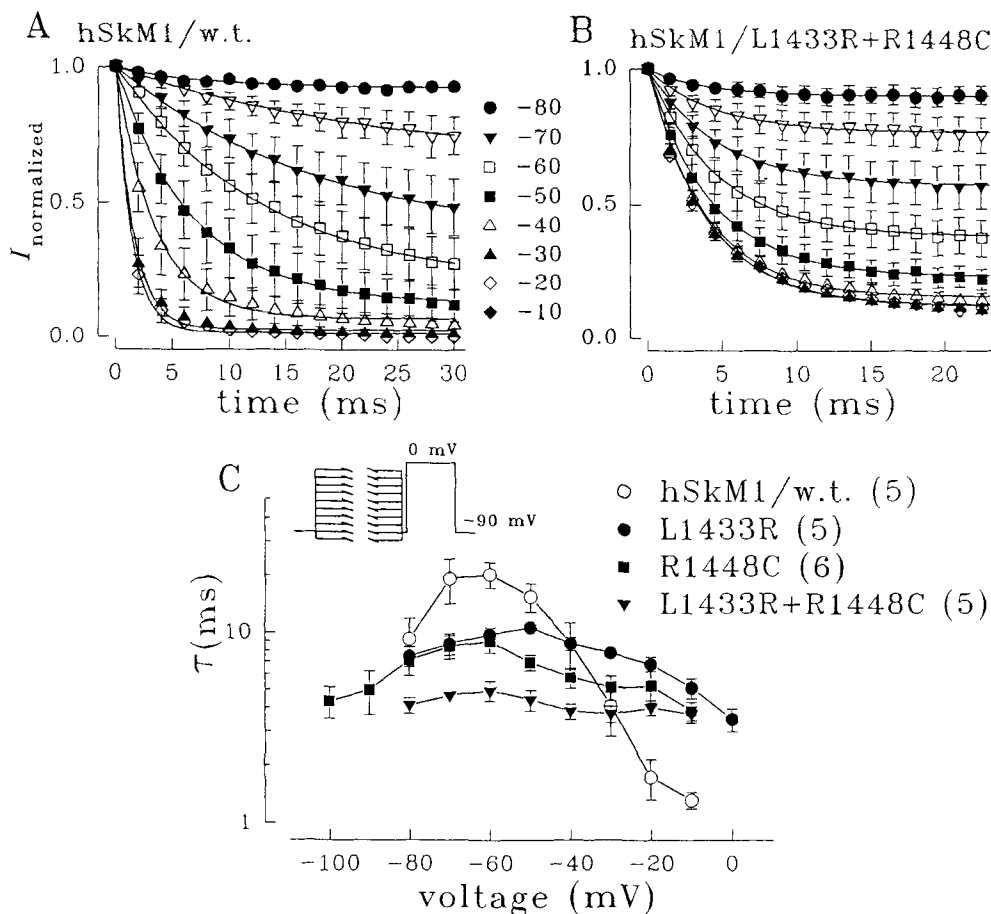
FIGURE 5. Effects of double mutation, L1433R and R1448C on conditioned inactivation. (A and B) Normalized peak currents of hSkM1/wt and double mutant channels, measured at a test potential of −10 mV after conditioning pulses (inset). Solid curves are the best fits of the data to a single exponential relaxation. Data from L1433R and R1448C mutant channels are not shown. (C) Time constants of conditioned inactivation in wild-type and mutant channels. Time constants were obtained by fitting data to a single exponential relaxation. All three mutants had smaller time constants at the membrane potentials at which no significant activation occurs.

L1433R and R1448C Mutations Affect hSkM1 Inactivation Differently

The naturally occurring mutation L1433R in D4/S3 slows inactivation, similar to the effect produced by other PC mutations (Yang et al., 1994). However, unlike the R1448C/H mutations, L1433R does not abolish the voltage dependence of τ_h at negative voltages (−40 to 0 mV), but increases τ_h values rather uniformly over the entire voltage range (Fig. 1 B), suggesting that the coupling of inactivation to activation (Armstrong and Bezanilla, 1977) is not lost in this mutation. L1433R apparently destabilizes an inactivated conformation, since it (a) increases τ_h, (b) decreases the time constant for recovery from inactivation (τ_{rcv}), and (c) shifts the steady state inactivation to more depolarized voltages. We postulate that the D4/S3 segment interacts with D4/S4, which is thought to play a more direct role in activation-to-inactivation coupling (Chahine et al., 1994; Keynes, 1994; Chen et al., 1995). Mutations of L1433 may, therefore, affect inactivation by influencing the voltage-dependent conformational transitions of D4/S4. This idea is explored in more detail below.

The differences of L1433R and R1448C mutations on

inactivation are further reflected by the molecular mechanisms underlying their effects. Unlike R1448C/H mutations, the change of charge is not critical for the action of the L1433R mutation. Instead, a change in the hydropathy of the S3 mutation is more important (Fig. 1 and Table I). This is consistent with the hypothesis that D4/S4 acts as a voltage sensor mediating the coupling of inactivation to activation, while D4/S3 supports S4 movements by maintaining an optimal local environment required for these movements. Analysis of the properties of substitutions at residue 1433 shows that hydropathy is an important factor. The effect on slowing of τ_h at −10 mV by L1433A/M/E/K/Q/R (in the order of increasing potency) correlates with the relative position of these amino acids on a hydrophobicity scale (leucine, 3.8; alanine, 1.8; methionine, 1.9; glutamic acid, −3.5; lysine, −3.9; glutamine, −3.5; and arginine, −4.5; Kyte and Doolittle, 1982). The main exception is the substitution by glutamine, an amino acid less hydrophilic than arginine; however L1433Q and L1433R have similar effects on τ_h. This exception might be due to other steric properties of these residues, such as forming a hydrogen bond with an altered angle (Jeffrey and Maluszynska, 1982). A change in the size of

A hSkM1/w.t.

5 ms

1 nA

10 ms

0 mV

−90 mV

B L1433R+R1448C

0.5 nA

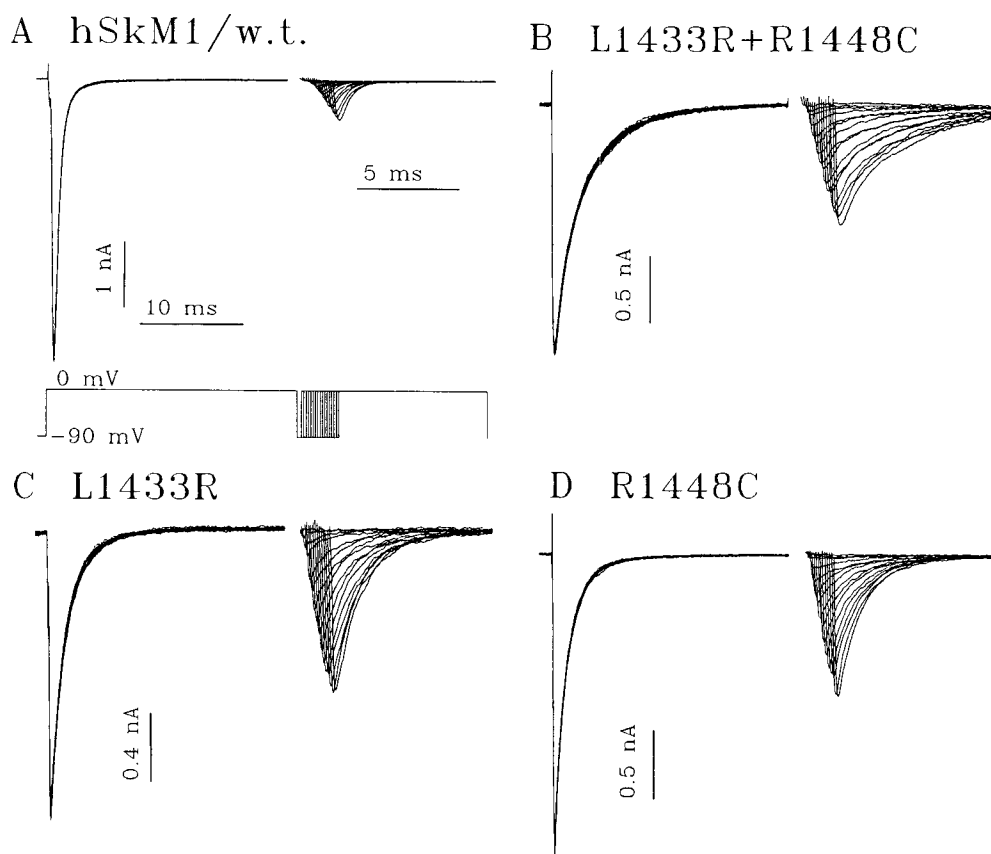C L1433R

0.4 nA

D R1448C

0.5 nA

FIGURE 6. Currents during recovery from inactivation. Current was recorded using a double pulse protocol (see inset). Shown in the figure were the currents recorded at a holding potential of −90 mV from wt, L1433R, R1448C, and double mutation. Note that current recovery begins with a greater delay in wt channels than in mutant channels.

the amino acid side chain is less crucial for the effects of L1433R, since the magnitude of the changes of τ_h produced by L1433A/M/E/K/Q/R does not match the change of Van der Waals volume of these amino acids (leucine, 124 Å³; alanine, 67 Å³; methionine, 135 Å³; glutamic acid, 109 Å³; lysine, 124 Å³; glutamine, 114 Å³; and arginine, 148 Å³; Creighton, 1993), except for the L1433A/R mutations.

While many factors are important for normal protein structure, the fact that the L1433K/E mutations affect inactivation similarly excludes the possibility that L1433R alters channel packing by forming additional salt bridges with adjacent acidic amino acids. This also excludes the possibility that addition of a charge to residue 1433 directly involves the electrostatic network inside the protein, which is thought to be important in maintaining the structure of *Shaker* potassium channels (Papazian et al., 1995). A possible mechanism by which L1433K/E mutations affect inactivation is the disruption of a hydrophobic interaction with residues of D4/S4.

D4/S3 and D4/S4 Effects on Inactivation Segregate with Voltage

The double mutant (L1433R+R1448C) resembles R1448C at voltages more depolarized than −40 mV (τ_h;

Fig. 4 *B*) and L1433R at more hyperpolarized voltages (τ_{rcv} and h_∞; Fig. 4, *C* and *D*). These kinetic and steady state measurements suggest that at depolarized voltages conformational transitions involving D4/S4 are rate limiting, whereas at more negative voltages D4/S3 conformation plays a primary role in inactivation. This voltage-dependent segregation of function may reflect the fact that at more hyperpolarized potentials we are primarily measuring transitions between closed and inactivated states, whereas at depolarized voltages τ_h is derived only from channels that have opened. This view is supported by the fact that R1448C has a much greater effect, at −20 mV, on inactivation from an open state than from closed states (Chahine et al., 1994). Our data also suggest that D4/S3 could be partly responsible for the fact that sodium channels tend not to open while they recover from inactivation (Kuo and Bean, 1994), but rather recover directly into closed states. This is consistent with a "first in, last out" principle. Large depolarizations cause an outward movement of D4/S4, followed by a rapid conformational change in D4/S3. These conformational transitions accompany inactivation. During recovery, D4/S4 cannot return to its resting conformation until D4/S3 undergoes a rate-limiting conformational change.

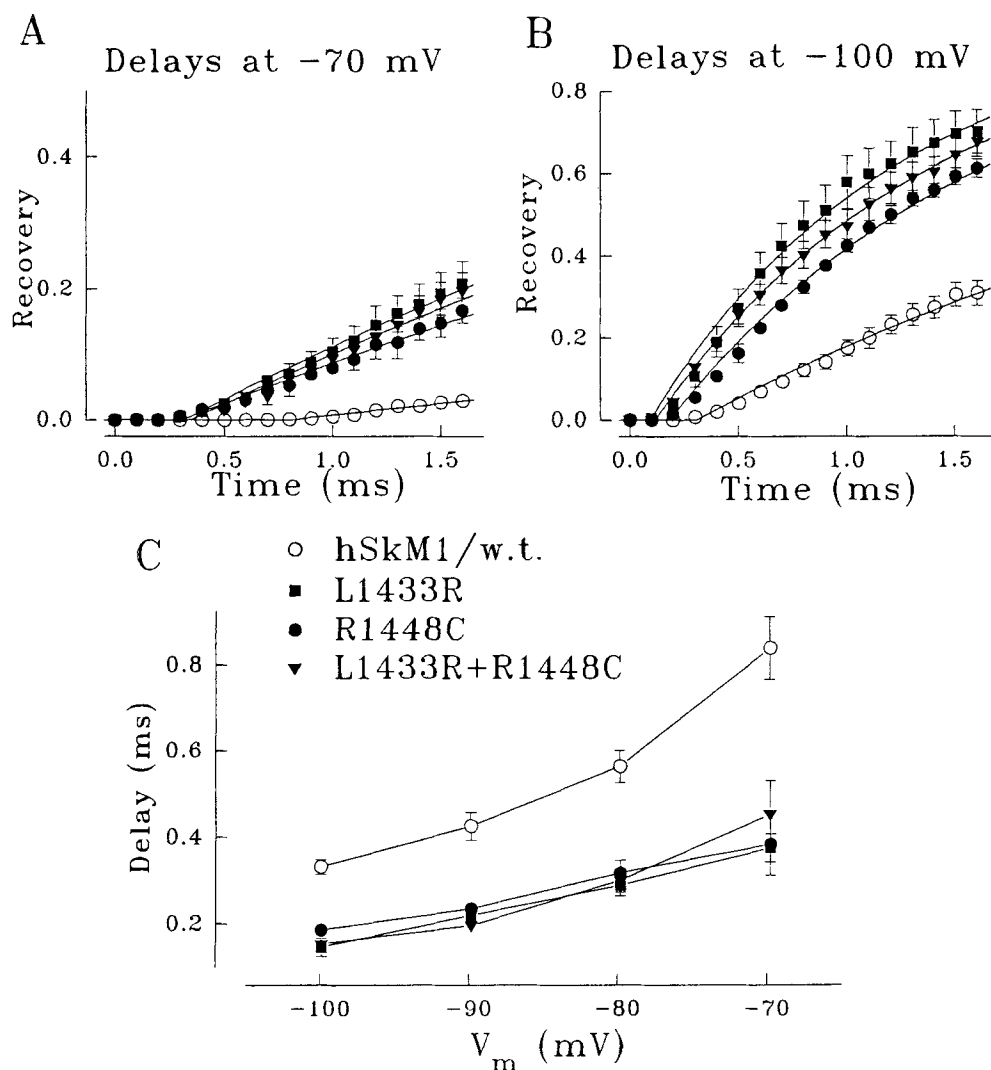The nonadditive nature of the effects of the point

A Delays at −70 mV

B Delays at −100 mV

C

○ hSkM1/w.t.
■ L1433R
● R1448C
▼ L1433R+R1448C

FIGURE 7. Voltage-dependence of the delay in recovery from inactivation. (*A* and *B*) Normalized currents recorded from recovery potentials of −70 and −100 mV. Solid curves are best fits to a single exponential with a delay. The delay is shorter at −100 mV than at −70 mV. Currents recorded at −80 and −90 mV are not shown. (*C*) Delays at different holding potentials. All three mutations shorten the delay in recovery similarly.

mutations strongly suggests that S3 and S4 interact during inactivation and recovery from inactivation. For example, if D4/S4 moves outward in response to depolarization (Yang and Horn, 1996), it may slide past D4/S3. Our data cannot, however, determine whether all of the effects of the L1433R mutation are secondary to its influence on D4/S4 movements. We have made one measurement that spans a voltage range from −80 to −10 mV, namely the rate of two-pulse inactivation (Fig. 5). For these data neither the S3 nor S4 mutation has a dominant action, since the double mutant differs from each of the single mutations. This may be due to the fact that two-pulse inactivation, unlike τ_h measurements, does not discriminate between closed and open channels (O'Leary et al., 1995).

To summarize the effects of the double mutation, we propose the following: a D4/S4 transition plays a rate-limiting role in the inactivation of channels at depolarized voltages, especially open channels. The state of D4/S3 is critical for inactivation at more negative volt-

ages, where transitions occur primarily between closed and inactivated states. Therefore, the unique biophysical properties of inactivation in the double mutant depend strongly on the state of the activation gates.

Relationship between Deactivation and Recovery from Inactivation

Our single and double mutations affect both the delay in recovery from inactivation and the kinetics of the tail currents (Figs. 7 and 8). It has been suggested that the delay in recovery is a consequence of the fact that deactivation (i.e., closing of activation gates) must precede recovery (Kuo and Bean, 1994). A similar delay precedes the onset of inactivation, and also may be due to the coupling of inactivation to activation (Bezanilla and Armstrong, 1977). Therefore, the delay in recovery and the decay of tail currents may both be a direct consequence of the backward movement of an activation voltage sensor. Fig. 7 shows that the delay in recovery is
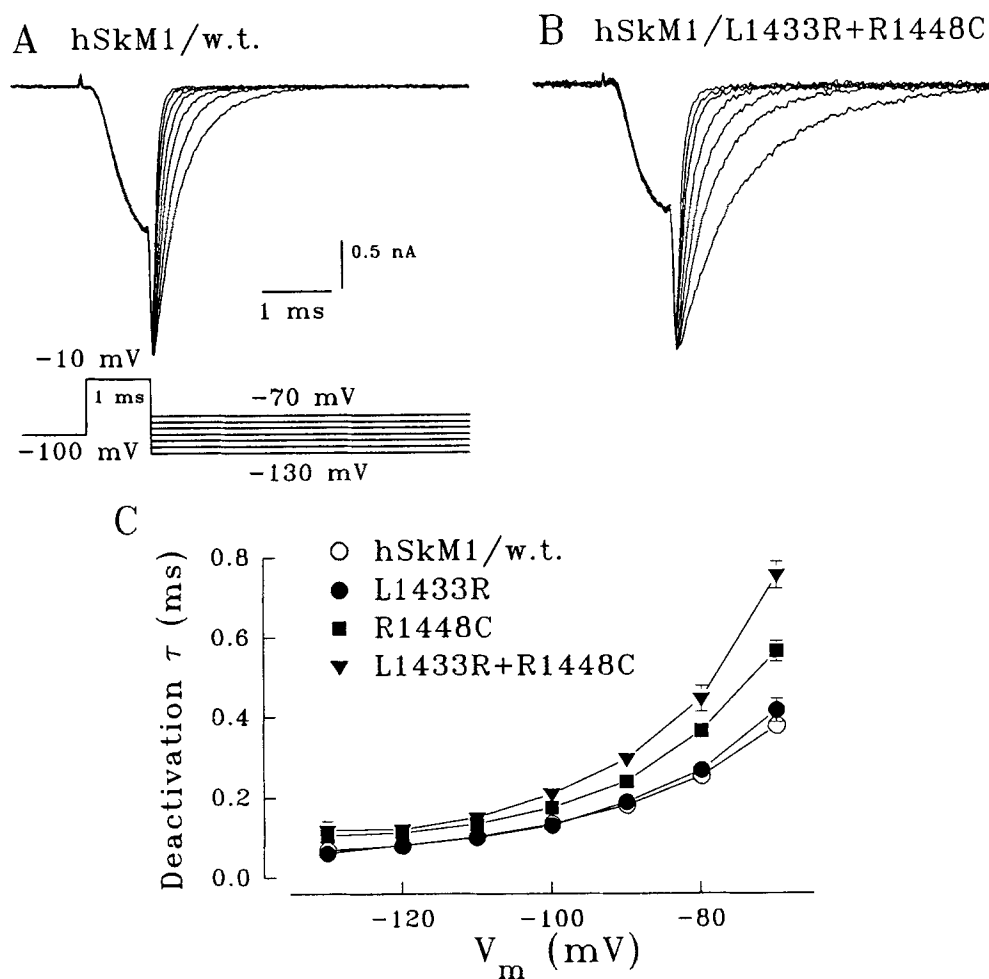
A hSkM1/w.t.

B hSkM1/L1433R+R1448C

0.5 nA

1 ms

−10 mV

1 ms

−70 mV

−100 mV

−130 mV

C

O hSkM1/w.t.
● L1433R
■ R1448C
▼ L1433R+R1448C

Deactivation τ (ms)

0.8
0.6
0.4
0.2
0.0

−120   −100   −80

V_m (mV)

FIGURE 8. Effects of mutant channels on the tail currents. Tail currents were recorded from −130 to −70 mV after a brief depolarization (1 ms) to −10 mV from a holding potential of −100 mV at 11.9°C. (A and B) show current traces recorded under these conditions from hSkM1/wt and double mutant channels. (C) Deactivation time constants. Deactivation time constants were estimated by fitting the decay of tail currents to a single exponential. Distinct from the effects on the delay in recovery, mutant channels affect tail current differently from each other.

abbreviated by mutations in both S3 and S4. However, the deactivation kinetics shown in Fig. 8 do not show the same pattern as the delay in recovery, since the tail currents are slowed by R1448C in S4 and not affected by L1433R in S3. The discrepancy may be explained by the fact that the rate of deactivation is affected by the state of the inactivation gate. If channels are open, L1433R has no effect on the rate of deactivation. The closing of the activation gate depends strongly, however, on the inward movement of D4/S4 (see Chahine et al., 1994 for other effects of R1448C on inactivation). By contrast, if channels are inactivated, mutations in both D4/S4 and D4/S3 may accelerate the closing of an activation gate, which is reflected as an abbreviated delay in recovery from inactivation. Therefore, D4/S3

can contribute to the closing of an activation gate only if the channel is inactivated. These data reveal the reciprocal nature of the interaction between activation and inactivation gates. The correlation between the delay and the deactivation should be further probed by examining the voltage dependence and time course of the delay and the remobilization of gating charge.

In summary, our data suggest that L1433R and R1448C mutations affect the gating of hSkM1 channels through distinct mechanisms. Segments D4/S4 and D4/S3 have different roles in hSkM1 channel gating. D4/S4 is more important in the deactivation and inactivation of open channels, whereas D4/S3 has a greater role in recovery of inactivated channels to a resting conformation.

REFERENCES

Armstrong, C. M., and F. Bezanilla. 1977. Inactivation of the sodium channel. II: Gating current experiments. *J. Gen. Physiol.* 70:567–590.

Barchi, R. L. 1995. Molecular pathology of the skeletal muscle sodium channel. *Annu. Rev. Physiol.* 57:355–385.

Bezanilla, F., and C. M. Armstrong. 1977. Inactivation of the sodium channel. I. Sodium current experiments. *J. Gen. Physiol.* 70: 549–566.

Blaber, M., X.-J. Zhang, and B. W. Mathews. 1993. Structural basis of amino acid α helix propensity. *Science (Wash. DC).* 260:1637–1640.

Cannon, S. C., and S. M. Strittmatter. 1993. Functional expression of sodium channel mutations identified in families with periodic paralysis. *Neuron.* 10:317–326.

Chahine, M., A. L. George, Jr., M. Zhou, S. Ji, W. Sun, R. L. Barchi, and R. Horn. 1994. Sodium channel mutations in paramyotonia congenita uncouple inactivation from activation. *Neuron.* 12:281–294.

Chen, L.-Q., V. Santarelli, P. Zhang, R. Horn, and R. G. Kallen. 1995. Unique role for the S4 segment of domain 4 of sodium channels. *Biophys. J.* 68:A156 (Abstr.).

Creighton, T. E. 1993. Proteins: structure and molecular properties. 2nd ed. W. H. Freeman and Company, New York.

Cummins, T. R., J. Zhou, F. J. Sigworth, C. Ukomadu, M. Stephan, L. J. Ptáček, and W. S. Agnew. 1993. Functional consequences of a Na⁺ channel mutation causing hyperkalemic periodic paralysis. *Neuron.* 10:667–678.

Durell, S. R., and H. R. Guy. 1992. Atomic scale structure and functional models of voltage-gated potassium channels. *Biophys. J.* 62: 238–250.

George, A. L. Jr., J. Komisarof, R. G. Kallen, and R. L. Barchi. 1992. Primary structure of the adult human skeletal muscle voltage-dependent sodium channel. *Ann. Neurol.* 31:131–137.

Guy, H. R., and P. Seetharamulu. 1986. Molecular model of the action potential sodium channel. *Proc. Natl. Acad. Sci. USA.* 83:508–512.

Hamill, O. P., A. Marty, E. Neher, B. Sakmann, and F. J. Sigworth. 1981. Improved patch-clamp techniques for high-resolution current recording from cells and cell-free membrane patches. *Pflügers Arch.* 391:85–100.

Horn, R., J. Patlak, and C. F. Stevens. 1981. Sodium channels need

not open before they inactivate. *Nature (Lond.).* 291:426–427.

Jeffrey, G. A., and H. Maluszynska. 1982. A survey of hydrogen-bond geometries in the crystal structures of amino acids. *Int. J. Biol. Macromol.* 4:173–185.

Ji, S., A. L. George, R. Horn, and R. L. Barchi. 1995. Sodium channel mutations and disorders of excitation in human skeletal muscle. *In* Ion Channels and Genetic Diseases. D. A. Dawson and R. A. Frizzell, editors. The Rockefeller University Press, NY. 61–76.

Keynes, R. D. 1994. The kinetics of voltage-gated ion channels. *Q. Rev. Biophys.* 27:339–434.

Kuo, C.-C., and B. P. Bean. 1994. Na⁺ channels must deactivate to recover from inactivation. *Neuron.* 12:819–829.

Kyte, J., and R. F. Doolittle. 1982. A simple method for displaying the hydropathic character of a protein. *J. Mol. Biol.* 157:105–132.

O'Leary, M. E., L.-Q. Chen, R. G. Kallen, and R. Horn. 1995. A molecular link between activation and inactivation of sodium channels. *J. Gen. Physiol.* 106:641–658.

Patlak, J. 1991. Molecular kinetics of voltage-dependent Na⁺ channels. *Physiol. Rev.* 71:1047–1080.

Papazian, D. M., X. M. Shao, S.-A. Seoh, A. F. Mock, Y. Huang, and D. Wainstock. 1995. Electrostatic interactions of S4 voltage sensor in *Shaker* K⁺ channel. *Biophys. J.* 68:A137 (Abstr.).

Ptáček, L. J., A. L. George, Jr., R. L. Barchi, R. C. Griggs, J. E. Riggs, M. Robertson, and M. F. Leppert. 1992. Mutations in an S4 segment of the adult skeletal muscle sodium channel cause paramyotonia congenita. *Neuron.* 8:891–897.

Ptáček, L. J., L. Gouw, H. Kwiecinski, P. McManis, J. R. Mendell, R. J. Barohn, A. L. George, Jr., R. L. Barchi, M. Robertson, M. F. Leppert. 1993. Sodium channel mutations in paramyotonia congenita and hyperkalemic periodic paralysis. *Ann. Neurol.* 33:300–307.

Yang, N., and R. Horn. 1995. Evidence for voltage dependent S4 movement in sodium channels. *Neuron.* 15:213–218.

Yang, N., S. Ji, M. Zhou, L. J. Ptáček, R. L. Barchi, R. Horn, and A. L. George, Jr. 1994. Sodium channel mutations in paramyotonia congenita exhibit similar biophysical phenotypes *in vitro*. *Proc. Natl. Acad. Sci. USA.* 91:12785–12789.